Inhalation Toxicology, 17:317–334, 2005

ISSN: 0895-8378 print / 1091-7691 online
DOI: 10.1080/08958370590929394

Taylor & Francis
Taylor & Francis Group

Dosimetric Adjustments for Interspecies Extrapolation of Inhaled Poorly Soluble Particles (PSP)

Annie M. Jarabek
National Center for Environmental Assessment, U.S. Environmental Protection Agency, Washington, DC, and CIIT Centers for Health Research, Research Triangle Park, North Carolina, USA

Bahman Asgharian and Frederick J. Miller
CIIT Centers for Health Research, Research Triangle Park, North Carolina, USA

Direct calculation of delivered dose in the species of interest potentially affects the magnitude of an uncertainty factor needed to address extrapolation of laboratory animal data to equivalent human exposure scenarios, thereby improving the accuracy of human health risk estimates. Development of an inhalation reference concentration (RfC) typically involves extrapolation of an effect level observed in a laboratory animal exposure study to a level of exposure in humans that is not expected to result in an appreciable health risk. The default dose metric used for respiratory effects is the average deposited dose normalized by regional surface area. However, the most relevant dose metric is generally one that is most closely associated with the mode of action leading to the response. Critical factors in determining the best dose metric to characterize the dose-response relationship include the following: the nature of the biological response being examined; the magnitude, duration, and frequency of the intended exposure scenario; and the mechanisms by which the toxicants exert their effects.

Dosimetry models provide mechanistic descriptions of these critical factors and can compute species-specific dose metrics. In this article, various dose metrics are postulated based on potential modes of action for poorly soluble particles (PSP). Dosimetry models are used to extrapolate the internal dose metric across species and to estimate the human equivalent concentration (HEC). Dosimetry models for the lower respiratory tract (LRT) of humans and rats are used to calculate deposition and retention using the principle of particle mass balance in the lower respiratory tract. Realistic asymmetric lung geometries using detailed morphometric measurements of the tracheobronchial (TB) airways in rats and humans are employed in model calculations. Various dose metrics are considered for the TB and pulmonary (P) regions. Because time is an explicit parameter incorporated in species-specific constants such as mucociliary clearance rates used in the models, the impact of the application of optimal model structures to refine adjustments and assumptions used in default risk assessment approaches to address exposure duration are discussed.

HEC estimates were found for particles ranging in sizes that corresponded to existing toxicity studies of PSP (0.3 to 5 μm). A dose metric expressed as number of particles per biologically motivated normalization factors (e.g., number of ventilatory units, number of alveoli, and number of macrophages) was lower than the current default of mass normalized to regional surface area for either deposited or retained dose estimates. Retained dose estimates were lower than

Received; accepted 19 January 2005.
This research was supported by a grant from the Long-Range Research Initiative of the American Chemistry Council. The authors are grateful to Drs. Owen Moss, Melvin Andersen, James Brown, and John Vandenberg for their critical reviews. We also thank Dr. Barbara Kuyper for her editorial assistance in the preparation of the article.

Address correspondence to Bahman Asgharian, CIIT Centers for Health Research, Six Davis Drive, PO Box 12137, Research Triangle Park, NC 27709-2137, USA. E-mail: basgharian@ciit.org

deposited dose estimates across all particle sizes evaluated. Dose metrics based on the deposited mass per unit area in small and large airways of the TB region indicate HECs of 1 to 5 times those of rats: that is, an equivalent exposure to humans which would achieve the same internal dose as in the rat would be 1 to 5 times greater. HEC estimates in the TB region increase with an increase in particle size for particles from 0.3 to ≤ 2 μm, then decrease with an increase in particle size for particles >2 μm in the small airways and >3 μm in the large airways. The HEC decreases with increase in particle size in the P region across all particle sizes studied, and the decrease has a more significant slope for those particles >2 μm due to the limited inhalability of particles this size in rats relative to humans.

Our modeling results elucidate a number of important issues to be considered in assessing current default approaches to dosimetry adjustment for inhaled PSP. Simulation of realistic, polydisperse particle distributions for the human exposure scenario results in reduced HEC estimates compared to estimates derived with the experimental particle distribution used in the laboratory animal study. Consideration should be given also to replacing the default dose metric of normalized deposited dose in the P region with normalized retained dose. Chronic effects are more likely due to retained dose and estimates calculated using retained versus deposited mass are shown to be lower across all particle sizes. Because dose metrics based on normalized particle number rather than normalized mass result in lower HEC estimates, use of inhaled mass as the default should also be revisited, if the pathogenesis suggests particle number determines the mode of action. Based on demonstrated age differences, future work should pursue the construction of "lifetime" estimates calculated by sequentially appending simulations for each specific age span.

When deriving health risk estimates of occupational or environmental inhalation exposures, toxicity data from laboratory animal inhalation studies are frequently extrapolated to estimate equivalent exposures to humans. The data from laboratory animal studies typically include rigorous exposure characterization and various measures of response in the target tissue. Interspecies extrapolation involves the application of several factors to the laboratory animal data. The need to address this extrapolation has been recognized by various national and international organizations (Bailey et al., 2003a; ICRP, 1994; U.S. EPA, 1994). The U.S. Environmental Protection Agency (EPA) employs a dosimetry adjustment to account for interspecies differences in delivered dose when extrapolating laboratory animal data to arrive at a human health estimate (U.S. EPA, 1994; Jarabek, 1995a, 1995c). This practice is best illustrated in the derivation of the reference concentration (RfC) as a health risk estimate (U.S. EPA, 1994; Jarabek, 1994, 1995a, 1995b; Bogdanffy & Jarabek, 1995). The RfC is defined as an exposure concentration for the general human population (including sensitive subpopulations) that is without appreciable risk of adverse noncancer health effects during a continuous, lifetime exposure.

The RfC methods use a hierarchal approach to dosimetry models employed for interspecies extrapolation (U.S. EPA, 1994; Jarabek, 1995c). Depending on the available information and understanding of the mode of action, a dosimetric adjustment factor (DAF) can range from a default algorithm to the use of a dosimetry model as the more optimal approach. Default adjustments require a limited number of parameters and are intended to provide a rudimentary but conservative (i.e., expected to be protective) description of delivered dose. In the case of respiratory effects due to inhaled particles, the default algorithm uses the average deposition mass fraction normalized to the respiratory tract region (extrathoracic or ET, tracheobronchial or TB, and pulmonary or P) in which the toxicity is observed (U.S. EPA, 1994; Jarabek, 1995c). The deposition fraction used in the default algorithm may be computed using empirical model descriptions of average particle deposition in each of the three respiratory-tract regions in various laboratory animals or humans (Miller et al., 1988; U.S. EPA, 1994; Ménache et al., 1995).

The hierarchal approach used in the RfC methods has been proposed to extend and "harmonize" dosimetry modeling across risk assessment approaches for noncancer versus cancer toxicity and for acute versus chronic exposures based on current emphasis on the utility of considering the mode of action in risk assessment (U.S. EPA, 1999; Wiltse & Dellarco, 2000; Jarabek, 2000; Bogdanffy et al., 2001). The dose metric should be described at a level of detail that is commensurate with both the level of detail used for the toxicity or nature of biological response under consideration and the intended duration of exposure for which the dose-response relationship is derived (U.S. EPA, 1994; Jarabek, 1995b, 1995c). The preferred models for dosimetric adjustment include species-specific and mechanistic determinants of chemical disposition and toxicant–target interaction to improve the accuracy of the dose-response description (Jarabek, 1995c).

A number of different dose metrics for inhaled poorly soluble particles (PSP) can be calculated, but the challenge is to select a dose metric that is mechanistically associated with or experimentally closely correlated to the biological response. Internal dose may be accurately described by particle deposition alone if the particles exert their primary action on the epithelial surface tissues (Dahl et al., 1991). For longer term effects, the initially deposited dose may not be as appropriate because particles clear at varying rates from different lung compartments so that some

dose is retained. To characterize chronic effects, models should calculate retained dose within the respiratory tract by accounting for clearance pathways.

Thus, the selection of a relevant dose metric for inhaled particles depends on whether a disease entity or adverse endpoint is better described by an acute or chronic pathogenesis process. The former disease process is more likely related to initial deposition and the latter to particle retention. For example, the acute mortality due to inhalation of particulate matter may relate more to recent deposited mass, while morbidity observed over long durations in some ecological epidemiological studies may relate more to retained mass (U.S. EPA, 1996; Snipes et al., 1997). A recent workshop on fiber and particle toxicity recommended that species-specific toxicokinetic models should be used to predict particle clearance and retention in the lungs (Greim et al., 2001).

Mechanistic insights on the role of specific properties in the pathogenesis and mode of action for particle toxicity can also be used to further refine the dose metric used in risk assessment applications. When different types of particles are compared, inhaled dose may be more appropriately expressed as particle volume, particle surface area, or number of particles rather than mass, depending on the toxic effect being evaluated (Oberdörster et al., 1994). Studies in rodents have shown that particle surface area is a better predictor than particle mass for both polymorphonuclear leukocyte (PMN) and tumor responses (Oberdörster, 1996; Driscoll et al., 1997; Tran et al., 2000a; Duffin et al., 2002). The retardation of alveolar macrophage-mediated clearance due to particle overload appears to be better correlated with phagocytized particle volume rather than mass (Morrow, 1988). Miller et al. (1995) performed simulations with a lung dosimetry model that suggested, particularly in patients with compromised lung status, the need to examine the role of particle number rather than mass for the fine fraction of aerosols in eliciting acute mortality and morbidity. Thus, different options for both the internal inhaled dose measure (e.g., mass or number) and the normalizing factor (e.g., surface area, alveolar macrophage) must be considered carefully in risk assessments for PSP.

This article describes dosimetry models for calculating various dose metrics for PSP, taking into account species-specific deposition and clearance processes in the lungs of humans and rats. Because hygroscopicity and solubility are not explicitly incorporated in the models used, this application is restricted to PSP. As defined by an International Life Sciences Institute (ILSI) workshop (ILSI, 2000), PSP are poorly soluble, nonfibrous particles that are of low toxicity and not directly genotoxic. A number of biologically relevant dose metrics are used to illustrate interspecies extrapolation and calculation of the human equivalent concentration (HEC). The different dose metrics vary based both on whether particle mass or number is used as the internal measure of dose and on the normalizing factor (e.g., ventilatory units, alveolar units, or alveolar macrophages). The explicit incorporation of exposure duration is also explored.

CALCULATION OF HUMAN EQUIVALENT CONCENTRATION (HEC)

The U.S. EPA RfC methods are currently the only regulatory risk assessment approach that routinely incorporates dosimetry adjustments. Efforts aimed at the harmonization of noncancer and cancer risk assessment approaches both use the RfC dosimetry methods as a platform and propose to extend the RfC methods with consideration of the mode of action (U.S. EPA, 1999; Wiltses Dellarco, 2000; Jarabek, 2000; Bogdanffy et al., 2001). Such an extension necessitates the consideration of additional dose metrics relevant to various potential biological mechanisms. We briefly review the derivation of the RfC to show how it can be derived for a specific dose metric and exposure scenario.

RfC calculations are described in detail elsewhere (Jarabek, 1994; U.S. EPA, 1994). To derive an HEC, the RfC methods apply the following to laboratory animal exposure data: an exposure duration adjustment, a DAF, and various uncertainty factors (UF). Our intention is to inspect the default time adjustment and DAF derivation, and then to show their relationship to estimates of delivered dose to the lung calculated using more mechanistic model structures.

The point of departure for the derivation of the RfC estimate is frequently based on laboratory animal data. The laboratory animal exposure concentration used in the derivation is typically a no-observed-adverse-effect level (NOAEL), a lowest-observed-adverse-effect level (LOAEL), or preferably an estimate obtained from a benchmark dose (BMD) approach (U.S. EPA, 1995). In the default derivation, a time adjustment is applied to account for the correction from the noncontinuous inhalation regimen in laboratory animal studies to an assumed continuous, lifelong exposure of 70 yr that is used as the target human exposure by:

$$\mathrm{NOAEL_{ADJ}} = \mathrm{NOAEL} \times \frac{H}{24} \times \frac{D}{7} \qquad [1]$$

where H, D, and $\mathrm{NOAEL_{ADJ}}$ designate hours per day, days per week, and the NOAEL that is duration adjusted from an intermittent exposure regimen to a continuous exposure level, respectively. The default duration adjustment is based on the premise that the product of the exposure concentration and duration of time ("$C \times t$" product) produces the same level of effect for a given endpoint (Haber, 1924). This adjustment is intended to be conservative (i.e., to be sufficiently protective of public health) and to account for the possibility that either the chemical or its damage can accumulate during chronic exposures (Jarabek, 1995b). However, this relationship is applicable only under limited exposure scenarios and conditions that may or may not include the case of PSP. Miller et al. (2000) showed that Haber's rule is a special case in a family of simple power law curves relating concentration and duration of exposure to response. Adherence to Haber's rule is seldom achieved for most biological endpoints because concentration is usually more important than duration of exposure in determining a given level of response. The relationship between exposure concentration

and duration also depends on what level of organization (e.g., an observation of the population, in the target tissue, or possibly in the subcellular domain of the genome or transcriptome) the endpoint is being observed (Jarabek, 1995c). The adverse toxic effect at any given level of organization is due to the internal dose at that level. For respiratory-tract effects, the quantitative pattern of deposition within the respiratory tract determines that dose as well as the specific pathways by which the inhaled material may be cleared and redistributed (Schlesinger, 1985). Because the various species used in inhalation toxicology studies that serve as the basis for dose-response assessment do not receive identical doses in a comparable respiratory-tract region when exposed to the same aerosol or gas, dosimetric adjustment for these intraspecies differences is requisite for accurate extrapolation of the dose response across species (Jarabek, 1995c).

A DAF is applied to determine the human equivalent exposure concentration as:

$$\mathrm{NOAEL_{HEC}} = \mathrm{NOAEL_{ADJ}} \times \mathrm{DAF} \qquad [2]$$

where $\mathrm{NOAEL_{HEC}}$ is the human equivalent exposure concentration to the NOAEL observed or chosen from the laboratory animal data. As shown next, the DAF is generally constructed of breathing parameters and target site deposition fraction in each species:

$$\mathrm{DAF} = \frac{(\dot{V}_\mathrm{E})_\mathrm{A}}{(\dot{V}_\mathrm{E})_\mathrm{H}} \times \frac{\mathrm{DF_A}}{\mathrm{DF_H}} \times \frac{\mathrm{NF_H}}{\mathrm{NF_A}} \qquad [3]$$

where $\dot{V}_\mathrm{E}$ is the minute ventilation, DF is the deposition fraction in the target site or region, and NF is the normalizing factor in humans (H) and animals (A). The default DF is derived from empirical models that describe average regional particle deposition as a function of particle diameter and distribution (Miller et al., 1988; Jarabek et al., 1989, 1990; Ménache et al., 1995). The NF for effects in the respiratory tract is often assumed to be the unit surface area of the target respiratory region (e.g., TB or P) or lung weight if thoracic deposition fraction is determined experimentally. Body weight is used as the default NF for remote (systemic effects) from inhalation exposures to particles.

The HEC for a lifelong exposure ($\mathrm{NOAEL_{HEC}}$) is converted to the RfC when adjusted by the application of uncertainty factors (UF) as:

$$\mathrm{RfC} = \frac{\mathrm{NOAEL_{HEC}}}{\mathrm{UF}} \qquad [4]$$

The underlying assumption in data extrapolation from laboratory animals to humans is that a human exposure that achieves an internal dose equivalent to that associated with a NOAEL observed for the critical effect in laboratory animals will be protective of public health. The composite UF can include a separate UF applied each for intrahuman variability, interspecies extrapolation, the use of a LOAEL instead of a NOAEL or benchmark dose, the use of data from a subchronic study rather than chronic bioassay data, and the use of an incomplete database that did not address all potentially relevant endpoints. Because the mechanistic motivations underlying some of these factors overlap, an RfC is not calculated when more than four of these areas of uncertainty are invoked in a derivation. When four factors are employed, the composite factor is constrained to be no greater than 3000 (Jarabek, 1994; U.S. EPA, 1994).

Improvements in human health risk estimates require mechanistic descriptions of particle fate and pathogenesis in the lung to both obtain more accurate estimates of the adjustment factors (time and dosimetric). Default UFs can then be replaced with data-driven values based on understanding the toxicant–target interactions underlying the mode of action. Improved descriptions of biologically effective internal doses are expected from models that include mechanistic determinants of both pharmacokinetic (PK) and pharmacodynamic (PD) components of the mode of action. Consideration of the adequacy of the characterization for PK and PD components is also the basis for the application of both the interspecies and intrahuman UF (Jarabek, 1995c). Thus, depending on the understanding of the toxicant–target interactions and pathogenesis, mechanistic model structures may also help to reduce the magnitude of UF applied for interspecies and intrahuman extrapolation.

Rearrangement of Eqs. (1–3) reveals that

$$\frac{\mathrm{NOAEL_{HEC}}}{\mathrm{NOAEL}} = \left[\frac{H}{24} \times \frac{D}{7} \times \frac{(\dot{V}_\mathrm{E})_\mathrm{A}}{(\dot{V}_\mathrm{E})_\mathrm{H}} \times \frac{\mathrm{DF_A}}{\mathrm{DF_H}}\right] \times \frac{\mathrm{NFH}}{\mathrm{NF_A}} \qquad [5]$$

Adjustment of exposure duration is inherent in the preceding expression in two instances. First, the intermittent regimen employed is duration adjusted by the "$C \times t$" product to a continuous exposure. Second, a chronic exposure (2-yr bioassay) is typically required as the basis for RfC derivation, and this duration is assumed to correspond to a lifetime human exposure scenario. If data from subchronic (90-day) animal studies are used as the basis instead, a UF is applied. It should be noted that the first adjustment essentially assumes equivalency of chronological time rather than physiological time between the two species, whereas ventilation rate is a physiological parameter that incorporates time implicitly. When more mechanistic models are used, additional parameters (e.g., clearance rates) also implicitly include physiological time. Computational capability is now such that dosimetry models can be used to calculate dose metrics in each species by simulating either exact exposure scenarios (e.g., applicable to acute emergency or occupational conditions) or steady-state conditions. Figure 1 illustrates the application of dosimetry models to perform interspecies extrapolation. The explicit exposure scenario for each species can be simulated with the dosimetry models to arrive at exposure estimates that result in comparable internal dose metric values. An alternative calculation that may also be informative is the simulation of the exact experimental regimen (e.g., 6 h/day for 5 days) in both laboratory animal and humans.

Exposure length can be explicitly inserted into Eq. (5) to obtain an equivalent exposure concentration between human and

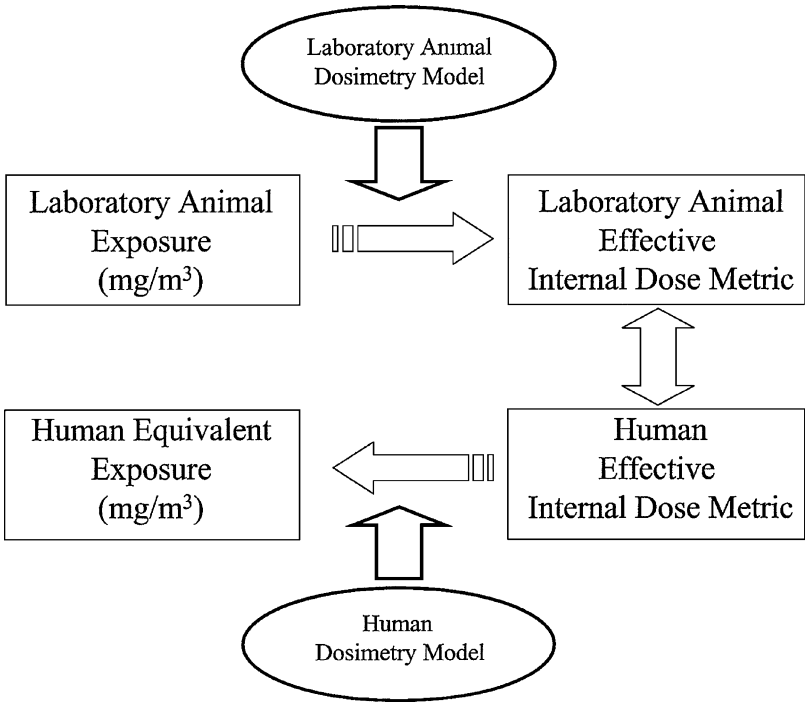

FIG. 1. Illustration of how a human equivalent concentration (HEC) is calculated from laboratory animal toxicity data using dosimetry/physiologically based pharmacokinetic (PBPK) models. An effective internal dose metric (e.g., the retained particle mass normalized to respiratory region surface area) associated with a key event or critical health effect at an administered dose (e.g., mg/m^3) is calculated by simulating the experimental exposure regimen (e.g., 6 h/day, 5 days/wk) for the laboratory animal. The human dosimetry/PBPK model is then used to simulate an exposure that achieves the same effective internal dose metric level using human parameters and exposure scenario assumptions (e.g., 24 h/day, 7 days/wk).

laboratory animal inhalation scenarios as:

$$\frac{\mathrm{HEC}}{C_\mathrm{A}} = \left[\frac{\delta t_\mathrm{A}}{\delta t_\mathrm{H}} \times \frac{(\dot{V}_\mathrm{E})_\mathrm{A}}{(\dot{V}_\mathrm{E})_\mathrm{H}} \times \frac{\mathrm{DF_A}}{\mathrm{DF_H}}\right] \times \frac{\mathrm{NF_H}}{\mathrm{NF_A}} \qquad [6]$$

where δt is the exposure duration and C_A is the laboratory animal exposure concentration such as the NOAEL.* Assuming, for example, the normalizing factor to be unit surface area of the target respiratory region, the terms inside the bracket can be combined to obtain a direct relationship between exposure concentration and deposition:

$$\frac{\mathrm{HEC}}{C_\mathrm{A}} = \frac{(\mathrm{Deposition/area})_\mathrm{A}}{(\mathrm{Deposition/area})_\mathrm{H}} = \frac{f[(\text{Adjusted depostion fraction, total minute volume, }\ldots)/\mathrm{area}]_\mathrm{A}}{f[(\text{Adjusted depostion fraction, total minute volume, }\ldots)/\mathrm{area}]_\mathrm{H}}. \qquad [7]$$

The exposure concentration, either the HEC or the laboratory animal concentration (C_A), is usually expressed as particle mass per volume of air because that is what has been historically sampled for exposure characterization. The DAF for interspecies extrapolation is expressed as a ratio of the chosen dose metric between species. To construct the ratio, various internal dose measures thought to address both the relevant physicochemical properties of the particles and the postulated pathogenesis of the critical effect of interest can be used. Thus, a given dose metric for a species used in construction of the ratio is the internal dose measure divided by the NF (dose metric = internal dose measure/NF). The internal dose measure could be the deposited fraction adjusted for hygroscopicity or solubility. The internal dose measure could also be just as well expressed as inhaled particle count, particle surface area, or some cumulative index relevant to the physicochemical property of the particles.

In general, the internal dose measure for humans and the laboratory animal species in Eq. (7) is assumed to be the same. That is, for any specific normalizing factor (e.g., number of

*C_A is used in place of NOAEL in this expression because the equations for dosimetric adjustment can be applied to either a NOAEL or lowest-observed-adverse-effect level (LOAEL). If a LOAEL were used, the RfC methods would require another UF.

alveolar macrophages), the proceeding expression can be further generalized to:

$$(\text{Dose metric})_H = (\text{Dose metric})_A. \quad [8]$$

The preferred approach for the use of a time adjustment and DAF is to consider a dosimetry model that integrates time-dependent processes directly into the calculation of the dose metric (Jarabek, 1995c; Bogdanffy & Jarabek, 1995; Bogdanffy et al., 2001).

RATIONALE AND APPROACH FOR DIFFERENT DOSE METRIC CALCULATIONS

As already discussed, laboratory animal bioassays are most often used to link exposure to biological outcomes. Measurements of the internal delivered dose are needed in the bioassay to allow interspecies extrapolation. However, the measured dose needed for the HEC or RfC calculation is either often lacking or the laboratory animal experiments are conducted with exposure scenarios that are incompatible with expected human exposure scenarios so that interspecies extrapolation is required. Dosimetry models can incorporate and integrate various parameters governing the fate of inhaled material in the lung and thus allow simulations of human and laboratory animal exposures to calculate the dose to the lung needed for the estimates of human exposure levels.

Most current dosimetry models are only capable of predicting particle deposition and clearance per lung region or specific site (e.g., Koblinger & Hofmann, 1985; ICRP, 1994; NCRP, 1997; Asgharian et al., 2001b). A new generation of dosimetry models has allowed site-specific dosimetry calculations (deposition plus clearance) with reasonable accuracy. Models have been developed in rats (Anjilvel & Asgharian, 1995) and humans (Asgharian et al., 2001a, 2001b) using realistic geometry of the lung derived from detailed, species-specific morphometric airway measurements. The models incorporate lung and breathing parameters to calculate airflow and particle transport within the respiratory tract to determine deposition and subsequent disposition.

DESCRIPTION OF THE DOSIMETRY MODELS

The particle dosimetry model applied herein is based on the following previously published work: Anjilvel and Asgharian (1995) for deposition in lung airways, Asgharian et al. (2001b) for mucociliary clearance in the TB region, and Asgharian et al. (2001c) for alveolar clearance. Details of the model structure and assumptions are provided therein. Briefly, the particle dosimetry model consists of a particle mass balance per airway that solves the connective–dispersion equation for an expanding and contracting airway. Due to the complexity of the airway geometry and its influence on airflow and deposition processes, several simplifying assumptions are made to allow a closed-form solution with a high degree of accuracy. These assumptions include the following: (1) Airflow travels uniformly with average parabolic velocity; (2) airflow to any airway is proportional to its distal volume; (3) particle losses at airway walls are represented in the mass-balance equations by deposition efficiency sink terms; and (4) axial diffusion and particle dispersion are neglected since these constitute second-order effects. The assumptions have been refined and validated by comparing predicted regional deposition estimates with other theoretical and numerical studies (Asgharian et al., 2001a).

The dosimetry models for humans and rats applied herein are available to the public as a software package known as multiple-path particle dosimetry (MPPD) (CIIT Centers for Health Research, 2004). The software uses a graphical user interface to aid computations and simulations required by toxicologists and risk assessors (Asgharian et al., 1999; Subramaniam et al., 2003). This application has used the latest version of MPPD issued in 2004 and is available upon request. A description of the software is available on the web at http://www.ciit.org/techtransfer/tt_technologies.asp. This same version of MPPD has been used in the companion application for the recent U.S. EPA assessment of particulate matter (U.S. EPA, 2004; Brown et al., this issue).

The MPPD model has the capability to calculate the deposition and clearance of monodisperse (geometric standard deviation σ_g of particle distribution ≤ 1.3) and polydisperse ($\sigma_g > 1.3$) aerosols in the respiratory tract of humans and rats for particles ranging from ultrafine (0.01 μm) to coarse (20 μm). The model is based upon "single-path" and "multipath" formalisms for tracking air flow and calculating aerosol deposition in the lung. The single-path method calculates deposition in a typical path per airway generation, while the multipath method calculates particle deposition in all airways of the lung to provide regional-, lobar-, and airway-specific estimates. Within each airway, deposition is calculated using theoretically derived efficiencies for deposition within the airway or airway bifurcation by the following mechanisms: diffusion, sedimentation, and impaction. Because PSP are the type of particle under consideration, the deposition calculations did not include an adjustment for hygroscopicity. Based on a mass balance of incoming, depositing, and exiting particles per airway, particle deposition fraction was found during a breathing cycle that included inhalation, pause, and exhalation.

Estimation and extrapolation of particle dose deposited in the lower respiratory tract (LRT) requires accurate assessment of the particles entering the respiratory tract; thus, particle inhalability and the filtration of aerosols by the head were taken into account. Particle inhalability is an important factor for interspecies extrapolation, given that particles inhalable by humans may only be partially inhalable by rats (U.S. EPA, 1994, 1996; Ménache et al., 1995). The empirical formulas for particle inhalability of Ménache et al. (1995) are the same as used in the empirical default model used by the U.S. EPA in the RfC methods. The filtering effects by the head to account for the proper fractional penetration of the inhaled aerosol reaching the LRT were also included. Analytical expressions given by Zhang and Yu (1993)

were derived based on measurements of particle depositions in the extrathoracic (ET) region of humans (Rudol et al., 1984) and F344 rats (Raabe, 1977, 1988).

The LRT geometry used for the single-path simulations in humans was based on the model of Yeh and Schum (1980) that comprised a typical-path symmetrical geometry. A five-lobe symmetric but structurally different geometry was used for the multipath simulations (Subramaniam et al., 2004). The geometry used in the model for rats was based on the data of Raabe et al. (1976) and consists of anatomical data for a comprehensive collection of the conducting airways of Long-Evans rats. The conducting airway structure in the rat model was complemented by attaching an eight-generation symmetric acinus structure (Yeh et al., 1979) to the end of each terminal bronchiole. The ventilatory and anatomical parameters used in the model calculations are provide in Table 1. The deposition component of the dosimetry model has been validated against experimental lung deposition measurements in humans and rats (Subramaniam et al., 2003; Anjilvels & Asgharian, 1995).

PSP were assumed to be insoluble and removed solely by particle clearance; dissolution was not an explicit term in the model. Two distinct clearance models were used: one for the TB region and another for the P region. Particle transport in the TB region was developed based on particle mass balance in each airway that included the following: particle deposition from inhaled air, influx from daughter branches (including those in the alveolar region), and removal by the mucociliary escalator. Transport equations for all the airways were solved simultaneously to calculate the retained mass in the conducting airways during exposure and postexposure times (Asgharian et al., 2001b).

In the conducting airways, clearance was assumed to occur primarily by mucociliary clearance. The TB clearance model is generic and applicable to any TB model structure for rats or humans once the mucous velocity in the trachea is specified. Mucous velocities were calculated for all conducting airways from the principle of mass balance using a tracheal mucous velocity of 5.5 mm/min in both rats and humans. Two assumptions were made for these calculations: (1) that the mucous layer traveled with an effective thickness that is small compared to airway diameter at a net constant velocity, and (2) that mucous production rates were the same in all the terminal bronchioles. Particle residence times were calculated based on mucous transport velocities in each airway. Transport equations for particles were solved numerically to estimate the retained mass (Asgharian et al., 2001b).

In the P region, the MPPD uses different clearance models for humans and rats. For humans, an analog of the International Commission on Radiological Protection (ICRP, 1994) compartmental model is used. The model is comprised of fast, medium, and slow compartments to describe the following: macrophage phagocytosis, physical particle translocation, and clearance to the lymph nodes via the alveolar interstitium. The clearance rates used for the fast (λ_{fast}), medium (λ_{med})s and slow (λ_{slow}) compartments were 0.02, 0.001, and 0.0001 day^{-1}, respectively. The slow compartment also clears via lymphatic channels (λ_L) at a rate of 0.00002 day^{-1}. Particle disposition in each alveolar region was found by first finding the summed alveolar deposition in each acinar region and then apportioning it to the fast (30%), medium (60%), and slow (10%) clearance compartments of the ICRP model. Particle removal from each alveolar (acinar) region was calculated independently. This led to a more accurate characterization of clearance than combining all the alveolar zones into one and then computing clearance for a single alveolar region.

In rats, a two-compartment model representing particle translocation along alveolar surfaces (λ_A) and to lymph nodes

TABLE 1
Anatomical parameters and ventilatory values for humans and rats used in the dosimetry model calculations

Species	URT volume (ml)	Functional residual capacity (FRC) (ml)	Minute ventilation (L/min)	Respiratory tract region[a]	SA (cm)^2	N_{VU}	N_{AV} (million)	N_{AM}[b] (million)
Human	50.0	3300.0	7.5	TB generations 1–13	1733			
				TB generations 14–21	2980			
				Entire TB	4713			
				Entire P	79,880	65,536	300	3630
Rat	0.42	4.0	0.214	TB generations 1–10	9.24			
				TB generations 11–41	11.44			
				Entire TB	20.68			
				Entire P	295.66	2404	30	45

Note. Upper respiratory tract (URT), surface areas (SA), number of ventilatory units (N_{VU}), and number of alveoli (N_{AV}) are calculated from the lung geometry of Asgharian et al. (2001a) for humans, and from the lung geometry of Anjilvel and Asgharian (1995) for rats.

[a]TB, tracheobronchial region; P, pulmonary region.

[b]Number of alveolar macrophages (N_{AM}) taken from Stone et al. (1992).

(λ_L) was attached to the end of each terminal bronchiole in each alveolar zone (Asgharian et al., 2001c). Lung burden measurements obtained from a 13-wk inhalation exposure of rats exposed to a monodisperse aerosol of pigmentary-grade TiO_2 (1.42 μm, $\sigma_g = 1.3$) at concentrations of 0, 10, 50, or 250 mg/m^3 (Bermudez et al., 2002) were used to calculate clearance-rate constants. An exponential function, mass-burden (m_A) dependent equation [$\lambda_A = 0.03341 \times \exp(-1.7759 m_A^{0.3123}) + 0.00071642$ mg/day] was fit to these data to calculate the overall alveolar clearance rate (λ_A) constants from the alveolar compartment. These rates were used in the clearance model to calculate particle transport. The assumed clearance rate from the alveoli to the lymphatic system (λ_L) is 0.00106 mg/day. The clearance model was verified using the data and models of Tran et al. (2000b) and Stöber et al. (1994) for a variety of other PSP.

DOSE METRIC EVALUATIONS

Because many toxicological bioassays are conducted in rats, dosimetry models of inhaled PSP for rats and humans were used to find HEC/C_A ratios in various regions of the respiratory tract based on various dose metrics. These dose metrics were calculated for a range of particle sizes that corresponds to existing toxicity studies of PSP (0.3 to 5 μm). Dose metrics calculated for the TB region included deposited mass normalized per unit surface area in bronchi (large airways), bronchioles (small airways), and the entire TB airways. Large and small airways were defined as generations 1 to 13 and 14 to 21 in humans, respectively; in rats these were defined as generations 1 to 10 and 14 to 21, respectively (see Table 1). Dose metrics in the P region were constructed using either mass or number as the internal dose with various NF. Dose metrics calculated for the P region included the following: the deposited mass normalized per unit surface area in the P region, and the number of particles deposited in the P region normalized per number of ventilatory units (N_{VU}), alveoli (N_{AV}), and alveolar macrophages (N_{AM}). In addition, dose metrics for the P region were calculated based on the retained mass during exposure periods of two different durations (4 and 26 wk).

Simple relationships can be derived when the dose metrics are based on net deposited mass as the internal dose measure. The deposited mass at a target site in the lung is calculated from

$$\text{Mass} = \text{DF} \times C \times \dot{V}_E \times \delta t \qquad [9]$$

Leaving the duration term in Eq. (9) explicitly to allow for different exposure scenarios between rats and humans results in the following for calculating the ratio of inhaled deposited mass in the lungs (NF_{PL} = per lung) of rats and humans:

$$\frac{\text{HEC}_{PL}}{C_A} = \frac{\delta t_A}{\delta t_H} \times \frac{(\dot{V}_E)_A}{(\dot{V}_E)_H} \times \frac{\text{DF}_A}{\text{DF}_H} \qquad [10]$$

where C_A is the exposure concentration for the laboratory animals. This term drops out if identical exposure scenarios are assumed (i.e., $\delta t_A = \delta t_H$). Note that the default "$C \times t$" adjustment term as in Eq. (5) is not used when dosimetry modeling is applied.

The following relationship prevails for a dose metric based on mass as the inhaled dose with surface area (SA) as the NF:

$$\left(\frac{\text{Mass}}{\text{SA}}\right)_H = \left(\frac{\text{Mass}}{\text{SA}}\right)_A \qquad [11]$$

Substituting for mass from Eq. (9) into Eq. (12) yields

$$\frac{\text{HEC}_{SA}}{C_A} = \frac{\delta t_A}{\delta t_H} \times \frac{(\dot{V}_E)_A}{(\dot{V}_E)_H} \times \frac{\text{DF}_A}{\text{DF}_H} \times \frac{\text{SA}_H}{\text{SA}_A} \qquad [12]$$

For dose metrics based upon the number of particles as the inhaled dose with N_{VU}, N_{AV}, or N_{AM} as the NF, the following relationships are obtained:

$$\frac{\text{HEC}_{VU}}{C_A} = \frac{\delta t_A}{\delta t_H} \times \frac{(\dot{V}_E)_A}{(\dot{V}_E)_H} \times \frac{\text{DF}_A}{\text{DF}_H} \times \frac{(N_{VU})_H}{(N_{VU})_A} \qquad [13]$$

$$\frac{\text{HEC}_{AV}}{C_A} = \frac{\delta t_A}{\delta t_H} \times \frac{(\dot{V}_E)_A}{(\dot{V}_E)_H} \times \frac{\text{DF}_A}{\text{DF}_H} \times \frac{(N_{AV})_H}{(N_{AV})_A} \qquad [14]$$

$$\frac{\text{HEC}_{AM}}{C_A} = \frac{\delta t_A}{\delta t_H} \times \frac{(\dot{V}_E)_A}{(\dot{V}_E)_H} \times \frac{\text{DF}_A}{\text{DF}_H} \times \frac{(N_{AM})_H}{(N_{AM})_A} \qquad [15]$$

where HEC may refer to number or mass concentrations. Of note is that Eq. (10) can be interpreted as a more general definition of DAF, and Eqs. (12) and (3) are identical but differ from Eqs. (13–15) in that the latter equations correspond to a DAF based on the number of particles deposited in various regions of the respiratory tract.

A simple relationship for DAF, similar to those represented by Eqs. (3) and (12), cannot be deduced when the dose metric is based on the retained mass in a region of the lung. In this case, a dosimetry model must be employed to calculate particle retention and related dose metrics for a region of the respiratory tract in humans and laboratory animals that explicitly incorporates the entire exposure scenario for each species. The dose metric based on retained mass can be described by a simple, first-order kinetic equation of the form:

$$\frac{dm/\text{NF}}{dt} = \dot{R} - \frac{\lambda m}{\text{NF}}$$
$$\dot{R} = \frac{\text{DF} \times \dot{V}_E \times C}{\text{NF}} \qquad [16]$$

where m is the retained mass, $\dot{R}$ is the normalized deposition rate, λ is the clearance rate constant, and C is exposure concentration. In a simulation of the experimental regimen for the rat, $C = C_A$; and when simulating human exposure scenarios, C = HEC. The retained mass arising from Eq. (16) is an accumulated mass for the simulated exposure period (e.g., 2 yr) and cannot be represented by an average daily dose. Instead, the mass burden from one day to the next is estimated by iterative application of Runga–Kutta methods.

Note that the duration adjustment applied in the default algorithm is obviated because the species-specific breathing pattern

and exposure scenarios used in dosimetry model simulations inherently include time adjustments. The models also allow exploration of assuming equal exposure periods between species (i.e., $\delta_A = \delta_H$) versus the default assumption of lifetime-equivalent, exposure concentration product periods (e.g., δ_A = a 2-yr, intermittent exposure regimen and $\delta_H = 70$ yr at a continuous level that is the "$C \times t$" equivalent to the intermittent regimen). The former may be more relevant to the evaluation of acute or occupational scenarios.

Finally, because the models incorporate physiological and anatomical factors that vary with age (e.g., ventilation and surface area), a set of simulations to explore interspecies extrapolation for different human age groups was performed. The dosimetry models were exercised using age-specific parameters in humans to evaluate their potential impact on the construction of "lifetime" human estimates.

RESULTS AND DISCUSSION

The dosimetry models just described were utilized to calculate various mechanistically motivated dose metrics for inhaled PSP deposited in the TB or P regions of rats and humans. Evaluation of the human equivalent concentration to rat exposure concentration (HEC/C_A) ratio between the species for these various dose metrics provides insights both on the dominant mechanisms underlying the internal dose in a particular species and on the adequacy of interspecies extrapolation using default algorithms for duration and dosimetry adjustment. The smaller the ratio, the lower is the equivalent resultant equivalent exposure level for humans.

The (HEC/C_A) ratios in the TB region were calculated from Eqs. (10–12) using the following dose metrics: total deposited mass normalized to total TB area, or deposited mass in the large versus small conducting airways normalized to their respective surface areas. Unit-density, monodisperse particles in the size range of 0.3 μm to 5.0 μm in diameter (thus, geometric or mass median aerodynamic diameter, MMAD) were used in the simulations.

The results for the various dose metrics based on deposition in the TB region are plotted in Figure 2. The HEC/C_A ratio rises slowly with particle diameter for particles smaller than 2 μm. Inhalability of particles >2 μm in diameter is 100% in humans but only about 85% in rats. Due to the limited inhalability of particles ≥ 2 μm in rats, the HEC begins to decrease with particle size >2 μm. The decrease for the HEC based on deposition in the small airways occurs for particles greater in diameter than about 2 μm and in the large airways for those greater than about 3 μm. The dose metrics based on mass per unit surface area are fairly close together in value for particles >2 μm in diameter. Significant deposition by impaction occurs for particles in the large airways of rats and humans for particles greater than about 2 μm. Based on a dose metric of inhaled mass per specific unit surface area, the HEC is about 1 to 5 times greater than the C_A. The HEC based on the current default (total deposited mass normalized to entire TB surface area) falls in the middle of

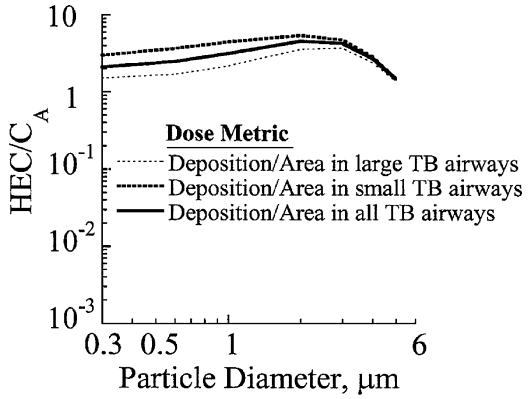

FIG. 2. Ratio of human equivalent concentration (HEC) to exposure concentration of the laboratory animal experiment (C_A) as a function of particle diameter (μm) for various dose metrics in the TB region. Simulations used unit density, monodisperse particles (thus, geometric or mass median aerodynamic diameter, MMAD). Laboratory animal species is the rat. Calculated dose metrics include the following: total deposited mass normalized to TB regional SA; and deposited mass in the large and small conducting airways, normalized to their respective surface areas.

estimates based on deposited mass in the large or small airways normalized to its respective surface area.

Potentially different pathogenesis processes with different biological outcomes may call for different dose metrics in the P region. Equations (11–15) were used to calculate the HEC/C_A ratio of various dose metrics based on deposited dose in the P region. The results for particle mass or number deposition (ignoring clearance processes) as the inhaled dose measure and normalized to SA, N_{AM}, N_{VU}, or N_{AV} as the dose metric are shown in Figure 3A. Due to the filtering effect and fractional penetration distally down the TB, the ratios in the P region decrease with increasing particle size and drop even more profoundly for particles that have limited inhalability in animals (i.e., particles >2 μm). The slopes of the lines for various dose metrics are almost identical. The range of HEC values for dose metrics based on the number of deposited particles normalized per macrophage, ventilatory unit, and alveolus spans only about one order of magnitude. A dose metric based on normalization per number of alveoli gives a lower value than a dose metric based on either normalization per number of ventilatory units or per number of alveolar macrophages. For the P region, use of dose metrics based on deposited particle number normalized to biologically motivated factors result in lower HEC estimates than the default (mass/SA) by a factor of 3.3 to 63 across the range of particle sizes evaluated.

Because the deposited particles reside in the LRT for extended periods of time, the likelihood is greater that injury or disease will correlate with retained dose (amount remaining with time) rather than with initial inhaled deposition. Thus, dose

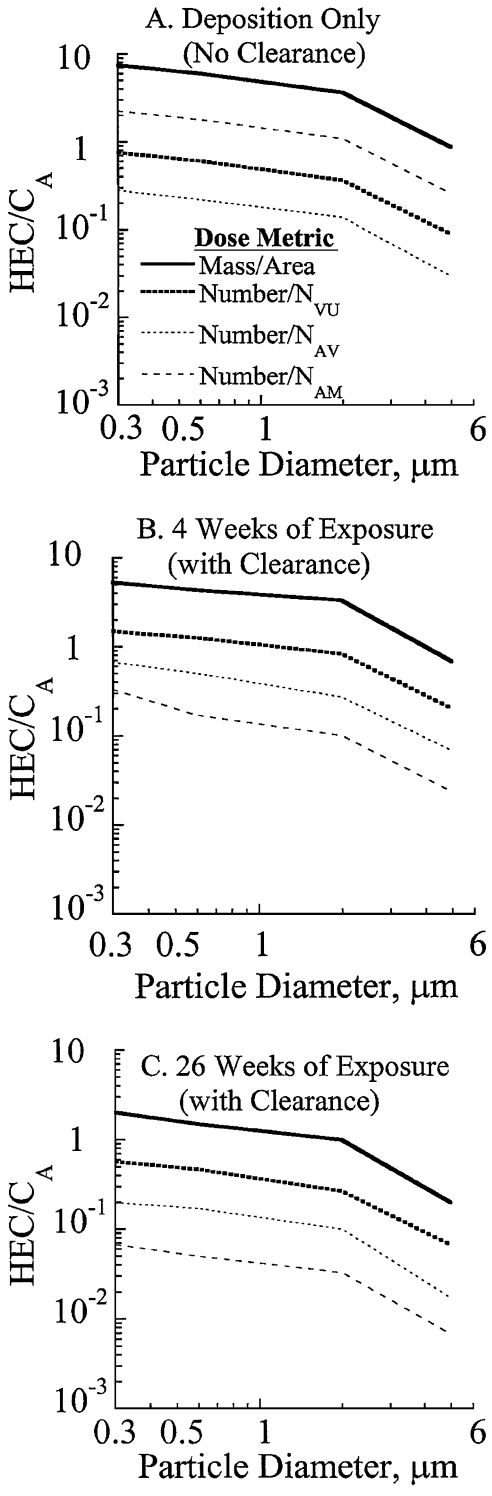

FIG. 3. Ratio of human equivalent concentration (HEC) to exposure concentration of the laboratory animal experiment (C_A) as a function of particle diameter (μm) for various dose metrics in the P region. Simulations for all exposures used unit density, monodisperse particles (thus, geometric or mass median aerodynamic diameter, MMAD). Laboratory animal species is the rat. For the 4-wk and 12-wk simulations, an intermittent regimen (6 h/day, 5 days/wk) and an exposure concentration of 30 μg/m^3 were used for the laboratory animal exposure; a continuous (24 h/day, 7 days/wk) exposure scenario was assumed for the human. (A) Results for initial deposition simulation. Calculated dose metrics include the following: total initially deposited (no clearance calculated) mass normalized by P regional SA, and initially deposited (no clearance calculated) number of particles normalized by various NF (N_{AM}, N_{VU}, N_{AV}). (B) Results for 4-wk exposure simulation. Calculated dose metrics include the following: retained mass normalized by P regional SA, and retained number of particles normalized by various NF (N_{AM}, N_{VU}, N_{AV}). (C) Results for 12-wk exposure simulation. Calculated dose metrics include the following: retained mass normalized by P regional SA, and retained number of particles normalized by various NF (SA, N_{AM}, N_{VU}, N_{AV}).

metrics based on retained dose in the P region of the LRT are more appropriate for extrapolation and evaluation of chronic exposures. Because particle removal from the P region is nonlinear with time and has unique kinetics in each species, simple relationships analogous to Eqs. (11)–(15) are not readily available to derive relationships between the HEC and C_A for retained dose metrics. Rather, an iterative procedure of simulations as discussed earlier is required to find the HEC (see also Figure 1).

For example, suppose that an exposure regimen of 6 h/day, 5 days/wk at a concentration of 30 μg/m^3 was employed in a rat inhalation study for 4 and 26 wk. Using clearance processes in the calculation, Figure 3B shows the results for the calculated HEC/C_A ratios after 4 wk of exposure for the different dose metrics in the P region; Figure 3C shows the calculated HEC/C_A ratios after 26 wk of exposure. All metrics based on retained dose show similar relationships as for deposition alone (Figure 3A): A dose metric based on retained mass per unit area gives a ratio with the highest value; a dose metric based on the number of particles retained in the P region per alveolus gives the lowest estimate. However, the value of the HEC/C_A ratio for the comparable retained mass dose metric is decreased at every particle diameter. The HEC/C_A ratios for the different dose metrics at 26 wk of exposure (Figure 3C) are lower than those for the 4-wk exposure (Figure 3B) by approximately two to six fold. This relationship implies that an even lower exposure level is required for humans to achieve the equivalent laboratory animal dose with increasing exposure duration, provided overload does not occur (Miller, 2000). A risk assessment extrapolating effects from chronic exposures in the P region should rely on dose metrics constructed using retained mass. Use of deposited mass for chronic exposures, as is the default practice, may lead to underestimation of risk to in humans due to PSP deposition and retention in the P region. Because particles in the TB region are generally cleared within 24 h, estimates for retained dose would not show dramatic time dependence so that dose metrics

based on deposited dose in the TB region are likely adequate for acute exposures.

To further study the effect of exposure regimen on the HEC/C_A ratios for retained dose metrics, two hypothetical cases based on existing inhalation exposure scenarios in the literature were simulated. The first case considered the scenario of a continuous, 24-h/day exposure at a concentration of 30 μg/m^3 for 3 days in both rats and humans. The results of the HEC/C_A ratios calculated from this scenario for various dose metrics in the P region are shown in Figure 4. The shapes, patterns, and trends for the dose metrics in Figure 4 are similar to those in Figure 3, B and C, but the HEC/C_A ratios are slightly higher than in Figure 3B.

For the second case, simulations were conducted of experimental exposures at various concentrations to polydisperse particles of different size distributions. Each particle distribution was defined by both the mass median aerodynamic diameter (MMAD) and geometric standard deviation (σ_g). Table 2 shows the resultant estimate of the HEC/C_A ratio for the different dose metrics. Relative to simulations of monodisperse particles, the various particle size distributions and exposure scenarios examined did not affect the relationships among the various P region dose metrics. However, the HEC/C_A ratios calculated for polydisperse particles differed from the estimates for monodisperse particles by about a factor of two fold less. Because polydisperse distributions are commonly found in the environmental

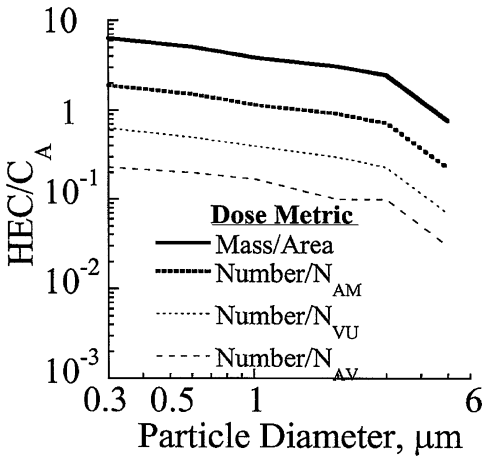

FIG. 4. Ratio of human equivalent concentration (HEC) to exposure concentration of the laboratory animal experiment (C_A) as a function of particle diameter (μm) for various dose metrics in the P region. Calculated dose metrics include the following: the retained particle mass normalized to P regional SA, and retained particle number with various NF (N_{AM}, N_{VU}, N_{AV}). Simulation used unit density, monodisperse particles (thus, geometric or mass median aerodynamic diameter, MMAD). Laboratory animal species is the rat. The simulation used an exposure regimen of 24 h/day for 3 days at a concentration of 30 μg/m^3 for both the rat and the human.

TABLE 2
Comparison of the calculated human equivalent concentrations (HEC) based on different dose metrics with experimental exposures concentrations in the rat (C_A)

							HEC/C_A		
							Dose metric is number of particles per		
	Exposure scenarios					Mass per unit area	Ventilatory unit (N_{VU})	Alveolus (N_{AV})	Alveolar macrophage (N_{AM})
Study	Strain/Treatment	Duration	Concentration (μg/m^3)	MMAD (μm)	σ_g				
Clarke et al. (1999)	Sprague-Dawley/ normal and bronchitic	5 h/day × 3 days	733	0.18	2.90	6.56	0.66	0.25	1.96
Killingsworth et al. (1997)	Sprague-Dawley/ Monochrotaline treated	6 h/day × 3 days	580	2.06	1.57	2.93	0.59	0.22	1.72
Kodavanti et al. (2000)	Spontaneously hypertensive rats	6 h/day × 3 days	15,000	1.95	2.14	2.87	0.29	0.11	0.85
Dormans et al. (1999)	Male Wistar	6 h/day ×5 days/wk × 4 wks	103,000	2.60	1.80	2.62	0.26	0.10	0.78

Note. Exposure scenarios quoted in the U.S. EPA Particulate Matter Criteria Document (2004) for various experimental studies conducted in laboratory animals. None of the studies indicated that these exposure levels induced overload.

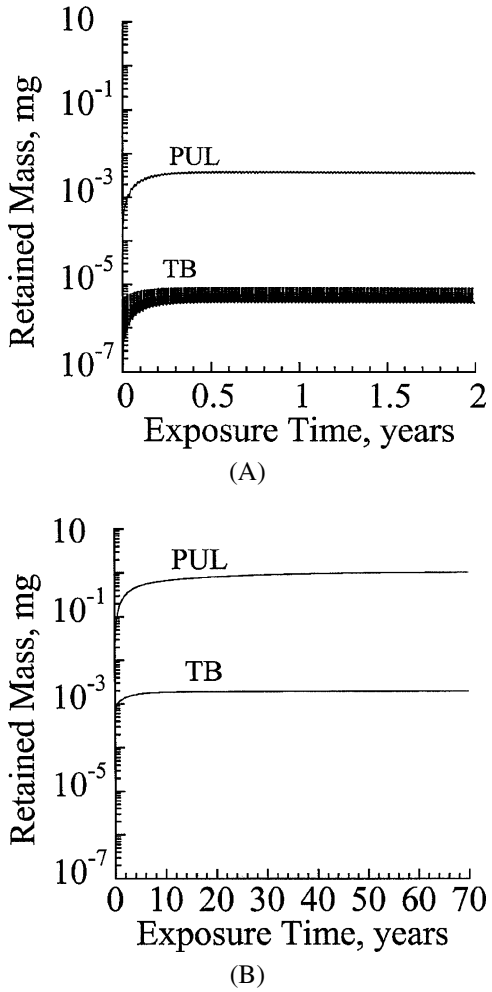

FIG. 5. Retained mass in the TB or P region normalized to regional surface area for two different human exposure scenarios. Both simulations used unit density, monodisperse particles (thus, geometric or mass median aerodynamic diameter, MMAD) at a concentration of 30 μg/m^3. Laboratory animal species is the rat. (A) Results for the simulation with a human exposure scenario that is identical to the intermittent regimen used in the laboratory animal study (6 h/day, 5 days/wk for 2 y). (B) Results for the simulation using the typically assumed, continuous exposure scenario (24 h/day, 7 days/wk, for 70 y) for humans.

conditions to which humans are exposed, simulations using actual aerosol characterization would have a similar impact on resultant risk estimates.

Two simulations shown in Figure 5 were used to explore the effect of assuming equal exposure periods between species (i.e., $\delta_A = \delta_H$) versus the default assumption of lifetime-equivalent, exposure-concentration product periods (i.e., δ_A = a 2-yr, intermittent exposure regimen and $\delta_H = 70$ yr at a continuous level that is the "$C \times t$" equivalent to the intermittent regimen). Particle diameter (1 μm of unit density) and exposure concentration (30 μg/m^3) were the same in each simulation. Using each exposure scenario, the retained mass normalized to surface area in the TB or P region was calculated for humans. Figure 5A shows the retained, normalized mass in humans for an exposure scenario that is identical to the regimen used in the laboratory animal study (6 h/day, 5 days/wk for 2 yr). Figure 5B shows the retained, normalized mass in humans for a typically assumed exposure scenario (24-h continuous, 7 days/wk, for 70 yr). The resulting pattern of the retained, normalized mass in each region is similar for both exposure simulations, indicating that periodicity of this internal dose metric would occur within the typical 2-yr time frame for the rodent bioassay. However, the end estimates at 2 yr versus 70 yr are quantitatively different by orders of magnitude in both the TB and P region. The difference in the retained, normalized mass estimates would be more pronounced for shorter-term exposures.

Figure 6A, and B, depicts the effect of the same two exposure scenarios assumed for Figure 5 on estimates of the HEC/C_A ratio versus particle diameter for dose metrics based on retained mass normalized to surface area in both the TB region (Figure 6A) and the P region (Figure 6B). Unit density, monodisperse particles (thus, geometric or mass median aerodynamic diameter, MMAD), and the same exposure concentration (30 μg/m^3) were used in each simulation. Using the assumption of an equivalent exposure scenario between rats and humans again results in lower HEC estimates across all particle diameters, by a factor of approximately 5 and 25 for the TB and P regions, respectively. The results of the simulations in Figures 4–6 should be given careful consideration in the development of dosimetry approaches for acute exposures. For example, across the particle diameters evaluated, differences between an HEC estimate based on retained mass in the P region as shown in Figure 4 (simulation of a 3-day continuous exposure in both species) versus as shown in Figure 6B (using the default human scenario) would be on the average about 166-fold higher.

The impact of exposure scenario assumption on the HEC/C_A estimate motivated another set of simulations to explore the effect of age. The human model was exercised for different age groups using anatomical parameters and ventilatory parameters specified in Asgharian et al. (2001a) and was used to calculate retained mass normalized to surface area. Unit-density, monodisperse particles (thus geometric or mass median aerodynamic diameter, MMAD) and the same exposure concentration (30 μg/m^3) were used in each simulation. The simulation was exercised until an apparent plateau was achieved for each age group. The age groups were chosen to represent a spectrum of time across which the lung continues to grow and change architecture. The minute ventilation values were 1.2, 2.9, 6.2, and 7.5 L/min for the 3-mo-old, 3-yr-old, 14-yr-old, and adult simulations, respectively. The TB surface area values were 206, 697, 1330, and 4713 cm^2 for the 3-mo-old, 3-yr-old, 14-yr-old, and adult (21-yr-old) simulations, respectively (Asgharian et al., 2004).

Figure 7 shows the results for the HEC/C_A ratio for various age groups versus particle diameter, using the retained mass in

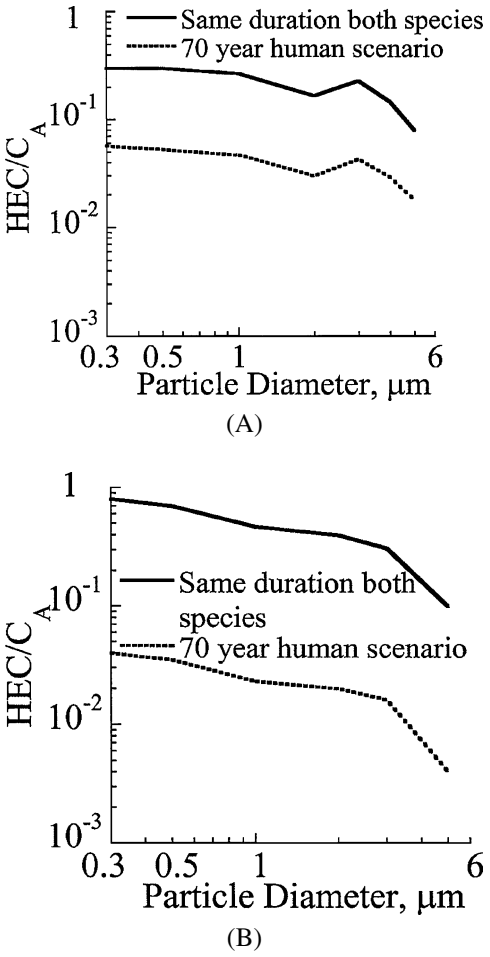

FIG. 6. The HEC/C_A ratio based on retained mass in the TB or P region normalized to regional surface area versus particle diameter for two different human exposure scenarios. Both simulations used unit density, monodisperse particles (thus, geometric or mass median aerodynamic diameter, MMAD) at a concentration of 30 μg/m^3. Laboratory animal species is the rat. The simulations in humans used either a human exposure scenario identical to the intermittent regimen used in the laboratory animal study (6 h/day, 5 days/wk for 2 y) or the typically assumed, continuous exposure scenario (24-h/day, 7 days/wk, for 70 y). (A) Results for the TB region. (B) Results for the P region.

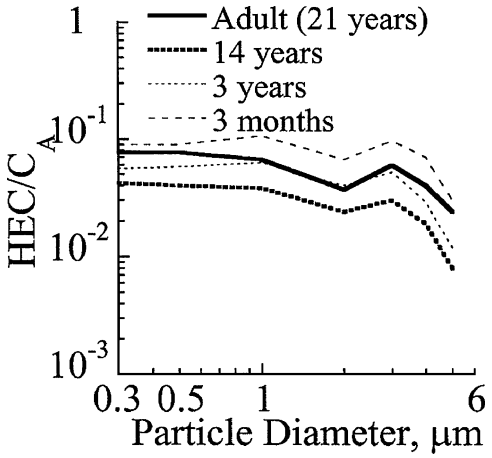

FIG. 7. The HEC/C_A ratio calculated using the retained mass in the TB region normalized to regional surface area as the dose metric. Calculations are shown for various age groups versus particle diameter. Simulations used unit density, monodisperse particles (thus, geometric or mass median aerodynamic diameter, MMAD) at a concentration of 30 μg/m^3. Laboratory animal species is the rat. The text provides the values of the anatomical and ventilatory parameters used in the simulations for each human age group.

the TB region normalized to surface area as the dose metric. The qualitative pattern is similar across all age groups. Because the resultant HEC/C_A ratio is lowest, the results suggest that the 14-yr-old may be at slightly greater risk than the adult. However, the differences in age groups appear to fall well within an order of magnitude and may be addressed by the typical, default 10-fold UF applied for intrahuman variability in both PK and PD. These results are similar to those estimated by Snipes et al. (1997) for retained mass in the P region of two different ambient aerosols. The differences by age group may well be due to changes in clearance as a function of age. Wolff (1992) showed that tracheal mucous velocity in beagle dogs increased to a maximum in young adults and then declined with age. Wolff (1992) also argued that age-related changes in canine lung function are similar to those changes in humans. Data on mucous velocities in children compared to those in human adults are needed to mechanistically characterize intrahuman variability.

Because the differences due to age may be more pronounced for other dose metrics, simulations should be developed to address age-specific risk. Another consideration for addressing differences in anatomical and physiological parameters at different age groups is that a true "lifetime" simulation should exercise the age-specific model for the appropriate duration (e.g., model simulation of the 3-mo-old followed by one for the next age interval) in a sequential fashion. Such a simulation is underway to estimate a "lifetime" cancer risk of formaldehyde using age-specific computational fluid dynamic (CFD) models for the upper respiratory tract (URT) and scaled age-specific models of the LRT to provide age-adjusted input to the clonal growth model developed by CIIT Centers for Health Research (Conolly et al., 2003, 2004; Kimbell et al., 2004). Such applications to address specific life stages are currently the topic of keen interest and likely to become more routinely applied in risk assessment as needed data are developed and associated dosimetry models evolve and mature (Clewell et al., 2004). The proposed "lifetime" calculation for PSP would be expected to make the largest difference for retained dose estimates.

CONCLUDING REMARKS

Risk assessment approaches typically require extrapolation of data from experimental studies in laboratory animals to estimate an HEC. Default approaches based on empirical models address dosimetry differences between species with some success in a rudimentary fashion, but nevertheless require application of UF to account for deficiencies in describing biological processes in an integrated fashion. More recent, sophisticated, mechanistic-dosimetry models offer an advantage in that they can both provide realistic simulations of specific exposure scenarios and also include determinants of airflow and particle transport processes in anatomically accurate geometries of human and rat lungs. Accounting for the mechanistic parameters is expected to increase the accuracy of interspecies extrapolation to an HEC. Recent emphasis on consideration of the mode of action in risk assessment is also more readily handled with these newer models because they allow potential dose metrics to be constructed for localized areas of the target respiratory tract regions. In addition, developing validated dosimetry models can offer tremendous time and cost savings. DAF can be generalized for a group of compounds similar in structure and expected mode of action. The dosimetry models used here embody such a generalization for the class of particles characterized as PSP (e.g., quartz, silica, diesel exhaust, titanium dioxide, carbon black) and can serve as a basis for the extension of models to address soluble and hygroscopic particles.

Mechanistic dosimetry models of particle inhalation, deposition, and clearance in humans and rats were used to simulate exposure scenarios of laboratory animal inhalation toxicity studies and various human exposure scenarios to calculate HEC estimates based on different dose metrics in the LRT. The various dose metrics were constructed considering plausible modes of action for PSP. These dose metrics included inhaled deposited and retained masses in various areas of the lung normalized to various factors that may be relevant to the mode of action (e.g., SA, N_{VU}, N_{AV}, N_{AM}). The results raise some important issues about the adequacy of current default approaches to interspecies dosimetric adjustment for exposures to PSP.

The explicit incorporation of time-dependent processes in dosimetry models allowed for evaluation of the assumption of a 24-h continuous exposure as the human exposure scenario. Using this assumption results in an HEC approximately an order of magnitude less than if an identical exposure is used for both the laboratory animal and human scenario. For example, the HEC using the default versus the similar scenario for an effect in the TB and PU region for an exposure of particles 1 μm in diameter would be 0.047 versus 0.27 and 0.023 versus 0.47, respectively. The results also confirm that this is a conservative assumption for chronic exposure evaluation and perhaps should be revised when attempting to address acute exposure risk. Further, the results also indicate the need to include more realistic exposure scenarios. Computational capacities are now readily capable of incorporating ventilatory activity patterns in dosimetry models. Such exercises have been used to support evaluation of the National Ambient Air Quality Standard (NAAQS) for particulate matter (U.S. EPA, 1996, 2004) and could be applied in the hazardous air pollutants arena as well (Snipes et al., 1997), Our results, as did others (U.S. EPA, 1996; Snipes et al., 1997), show that that the use of a realistic, polydisperse distribution in the human dosimetry models results in a lower HEC estimate. Thus accurate characterization of the particle size and distribution of the actual ambient exposure to which humans are exposed becomes a critical input.

Due to clearance within 24 h in the TB region, deposited mass per unit area is probably the relevant dose metric for effects in this region from acute exposures. More specific area-based dose metrics can be defined if the target site in the TB region is identified and the mode of action understood. In the P region, a preferred dose metric would be based on a normalized retained mass rather than a normalized deposited mass, notably for the evaluation of chronic exposures. The adverse effects of long-term exposures to PSP are more likely related to retained mass. PSP clearance is based primarily on mechanical transport processes that we demonstrate can be calculated from the available literature on mucociliary rates and clearance half-times.

Use of dose metrics based on the number of retained particles and normalized to the number of alveoli, macrophages, or ventilatory units all gave rise to different HEC estimates for the P region that varied by about an order of magnitude and that were all lower than those based on the current default of particle mass normalized to P surface area. The HEC based on the default versus the number dose metric was higher by a factor of about 3.0 to 4.0 when based on metric of number normalized to ventilatory units, to about 16 to 30 when based on the metric of number normalized to alveolar macrophages. Careful consideration should be given to these alternate dose metrics if the mode of action indicates that particle number may be more relevant to the pathogenesis of the effects under evaluation.

Analysis of age-dependent estimates indicates that the variability in TB-deposited mass across a span of 3 mo to adulthood is within an order of magnitude and may be addressed by the 10-fold UF typically applied for intrahuman variability. However, future work should pursue evaluation of other dose metrics in both lung regions and consider construction of "lifetime" estimates by sequentially appending simulations for each specific age span. Rather than a default factor applied to adult simulations, such a composite simulation would more accurately describe the mechanistic differences due to changes in lung function with age.

The mechanistic model simulations herein and the empirical models used with the default algorithm in the RfC methods are based on PSP (U.S. EPA, 1994). Key input parameters are particle diameter and distribution. Previous simulation exercises have shown that particle solubility rates are dominant determinants of

lung burdens for inhaled particles of ambient aerosols (Snipes et al., 1997). Therefore, data on dissolution rates become a key research need to address (Snipes et al., 1997; Bailey et al., 2003b) in order to extend these models to additional types of particles. Nevertheless, it is expected that taking into account inhalability and deposition efficiency does address to some degree the key determinants of interspecies differences in inhaled dose. Indeed, Cassee et al. (2003) showed that the MPPD adequately predicts lung burdens of a soluble cadmium chloride aerosol in rats. Thus the current default of normalized mass of PSP used by the U.S. EPA (1994) is supported. Future work should evaluate refinements due to the incorporation of strain differences (DeLorme & Moss, 2002) and hygroscopicity (Schroeter et al., 2001; Asgharian, 2004). Because the mouse is the species used in many genomic evaluations, mechanistic models to improve the empirical ones that currently estimate only deposition should be encouraged.

Additional data needed to develop and extend the models for a specific assessment application are information on the nature of toxicity of the particle under evaluation, for example, genotoxicity. Careful characterization of the activity diameter would also be useful (U.S. EPA, 1994). This expression takes into account the "activity" of the physical property of the particle. For example, if the toxicant is distributed only on the surface, then the activity median diameter is equal to the surface median diameter (U.S. EPA, 1994). Further discussion of issues related to activity diameters can be found elsewhere (Hofmann & Koblinger, 1989). Because particle distributions are assumed to be lognormal, estimation of count, surface area, or volume distributions for any given sample of particles can be made after one of those distributions has been measured using equations originally derived by Hatch and Choate (1929). Additional discussion of particle diameter definitions and conversions can also be found elsewhere (U.S. EPA, 1994; Moss & Cheng, 1989).

The application of dosimetry models represents a refinement and extension of the existing default RfC methods based on the average deposited mass normalized to regional surface area. We used these models to calculate different doses to various local targets within the lungs of humans and rats. Once developed, physiologically based pharmacokinetic (PBPK) models can be used to describe toxicant–tissue reactions in greater detail. Further refinements can be expected with the development and validation of models that predict more localized estimates in the P region. Disease-based models will provide insight on potential susceptibility, such as differences in deposition and retention due to the effects of altered geometry on airflow (Segal et al., 2002). Differences in ventilation/perfusion (V/Q) mismatch and perfusion may prove to be important to systemic delivery of toxic moieties. Finally, the LRT models are also a valuable complement to models that predict localized deposition in the upper respiratory tract (URT) (Kimbell et al., 2001). Use of dosimetry models of the URT and LRT together affords more accurate approaches for both interspecies extrapolation and the characterization of intrahuman variability in the entire respiratory tract.

REFERENCES

Anjilvel, S., and Asgharian, B. 1995. A multiple-path model of particle deposition in the rat lung. *Fundam. Appl. Toxicol.* 28:41–50.

Asgharian, B. 2004. A model of deposition of hygroscopic particles in the human lung. *Aerosol Sci. Technol.* 38:938–947.

Asgharian, B., Hofmann, W., and Bergmann, R. 2001a. Particle deposition in a multiple-path model of the human lung. *Aerosol Sci. Technol.* 34:332–339.

Asgharian, B., Hofmann, W., and Miller, F. J. 2001b. Mucociliary clearance of insoluble particles from the tracheobronchial airways of the human lung. *J. Aerosol Sci.* 32:817–832.

Asgharian, B., Wong, B. A., Bermudez, E., and Everitt, J. I. 2001c. A model of clearance of titanium dioxide from the rat lung. *Toxicologist* 60(1):195.

Asgharian, B., Kelly, J. T., and Tewksbury, E. W. 2003. Respiratory deposition and inhalability of monodisperse aerosols in Long-Evans rats. *Toxicol. Sci.* 71:104–111.

Asgharian, B., Ménache, M. G., and Miller, F. J. 2004. Modeling age-related particle deposition in humans. *J. Aerosol Med.* 17(3):213–224.

Bailey, M. R., Ansoborlo, E., Guilmette, R. A., and Paquet, F. 2003a. Practical applications of the ICRP human respiratory tract model. *Radiat. Protect. Dosim.* 105(1–4):71–76.

Bailey, M. R., Ansoborlo, E., Camner, P., Chazel, V., Fritsch, P., Hodgson, A., Kreyling, W. G., Le Gall, B., Newton, D., Paquet, F., Stradling, N., and Taylor, D. M. 2003b. RBDATA-EULEP: Providing information to improve internal dosimetry. *Radiat. Protect. Dosim.* 105(1–4):633–636.

Bermudez, E., Mangum, J. B., Asgharian, B., Wong, B. A., Reverdy, E. E., Janszen, D. B., Hext, P. M., Warheit, D. B., and Everitt, J. I. 2002. Long-term pulmonary responses of three laboratory rodent species to subchronic inhalation of pigmentary titanium dioxide particles. *Toxicol. Sci.* 70:86–97

Bogdanffy, M. S., and Jarabek, A. M. 1995. Understanding mechanisms of inhaled toxicants: implications for replacing default factors with chemical-specific data. *Toxicol. Lett.* 82/83:919–932.

Bogdanffy, M. S., Daston, G., Faustman, E. M., Kimmel, C. A., Kimmel, G. L., Seed, J., and Vu, V. 2001. Harmonization of cancer and noncancer risk assessment: Proceedings of a consensus-building workshop *Toxicol. Sci.* 61:18–31.

Cassee, F. R., Muijser, H., Duistermaat, E., Freijer, J. J., Geerse, K. B., Marijnissen, J. C. M., and Arts, J. H. E. 2002. Particle-size dependent total mass deposition in lungs determines inhalation toxicity of cadmium chloride aerosols in rats. Application of a multiple path dosimetry model. *Arch. Toxicol.* 76:277–286.

CIIT Centers for Health Research. 2004. Multiple path particle dosimetry model MPPD, v. 2.0.

Clarke, R. W., Catalano, P. J., Koutrakis, P., Krishna, M. G. G., Sioutas, C., Paulauskis, J., Coull, B., Ferguson, S., and Godleski, J. J. 1999. Urban air particulate inhalation alters pulmonary function and induces pulmonary inflammation in a rodent model of chronic bronchitis *Inhal. Toxicol.* 11:637–656.

Clewell, H. J., Gentry, P. R., Covington, T. R., Sarangapani, R., and Teeguarden, J. G. 2004. Evaluation of the potential impact of

age- and gender-specific pharmacokinetic differences on tissue dosimetry. *Toxicol. Sci.* 79:381–393.

Conolly, R. B., Kimbell, J. S., Janszen, D., Schlosser, P. M., Kalisak, D., Preston, J., and Miller, F. J. 2003. Biologically-motivated computational modeling of formaldehyde carcinogenicity in the F344 rat. *Toxicol. Sci.* 75:432–447.

Conolly, R. B., Kimbell, J. S., Janszen, D., Schlosser, P. M., Kalisak, D., Preston, J., and Miller, F. J. 2004. Human respiratory tract cancer risks of inhaled formaldehyde: Dose-response predictions derived from biologically-motivated computational modeling of a combined rodent and human dataset. *Toxicol. Sci.* 8:1–18.

Dahl, A. R, Schlesinger, R. B., Heck, H.d'A., Medinsky, M. A., and Lucier, G. W. 1991. Comparative dosimetry of inhaled materials: Differences among animal species and extrapolation to man. *Fundam. Appl. Toxicol.* 16:1–13.

DeLorme, M. P., and Moss, O. R. 2002. Comparison of restrained and unrestrained whole-body plethysmographs for mice. *J. Pharmacol. Toxicol. Methods* 47:1–10.

Dormans, J. A. M. A., Steerenberg, P. A., Arts., J. H. E., Van Bree, L., De Klerk, A., Verlann, A. P. J., Bruijntjes, J. P., Beekhof, P., Van Soolingen, D., and Van Loveren, H. 1999. Pathological and immunological effects of respirable coal fly ash in male Wistar rats. *Inhal. Toxicol.* 11:51–69.

Driscoll, K. E., Deyo, L. C., Carter, J. M., Howard, B. W., Hassenbein, D. G., and Bertram, T. A. 1997. Effects of particule exposure and particle-elicited inflammatory cells on mutation in rat alveolar type II cells. *Carcinogenesis* 18:23–430.

Duffin, R., Tran, C. L., Clouter, A., Brown, D. M., MacNee, W., Stone, V., and Dondaldson, K. 2002. The importance of surface area and specific reactivity in the acute pulmonary inflammatory response to particles. *Ann. Occup. Hyg.* 46(suppl.1):242–245.

Ghio, A. J., Kim, C., and Devlin, R. B. 2000. Concentrated ambient air particles induce mild pulmonary inflammation in healthy human volunteers. *Am. J. Respir. Crit. Care Med*. 162:981–988.

Gong, H., Sioutas, C., Linn, W. S., Clark, K. W., Terrell, S. L., Terrell, L. L., Anderson, K. R., Kim, S., and Chang, M.-C. 2000. Controlled human exposures to concentrated ambient fine particles in metropolitan Los Angeles: Methodology and preliminary health-effect findings. *Inhal. Toxicol.* 12(suppl. 1):107–119.

Greim, H., Borm, P., Schins, R., Donaldson, K., Driscoll, K., Hartwig, A., Kuempel, E., Oberdörster, G., and Speit, G. 2001. Toxicity of fibers and particles—Report of the workshop held in Munich, Germany, 26–27 October 2000. *Inhal. Toxicol.* 13(9):737–754.

Haber, F. 1924. Zur geschichte des gaskrieges (On the history of gas warfare). In *Fünf Vorträge aus den Jahren 1920–1923 (Five lectures from years 1920–1923)*, pp. 76–92. Berlin: Springer.

Hatch, T., and Choate, S. P. 1929. Statistical description of the size properties of non-uniform particulate substances. *J. Franklin Inst.* 207:369–387.

Heyder, J., Beek-Speier, I., Busch, B., Dirscherl, P., Heilmann, P., Ferron, G. A., Josten, M., Karg, E., Kreyling, W. G., Lenz, A.-G., Maier, K. L., Miaskowski, U., Platz, S., Reitmeir, P., Schulz, H.. Takenaka, S., and Ziesenis, A. 1999. Health effects of sulfur-related environmental air pollution. I. Executive summary. *Inhal. Toxicol.* 11:343–359.

Hofmann, W., and Bergmann, R. 1998. Predictions of particle deposition patterns in human and rat airways. *Inhal. Toxicol.* 10:557–583.

Hofmann, W., and Koblinger, L. 1989. The effect of polydispersity of radioactive aerosols on the activity distribution in the human lung. *J. Aerosol. Sci.* 20:1313–1316.

International Commission on Radiological Protection. 1994. Human respiratory tract model for radiological protection. ICRP Publication 66. *Annals ICRP* 24:1–3.

International Life Sciences Institute. 2000. ILSI Risk Science Institute Workshop: The relevance of the rat lung response to particle overload for human risk assessment: A workshop consensus resport. *Inhal. Toxicol.* 12(1–2):1–17.

Jarabek, A. M. 1994. Inhalation RfC methodology: dosimetric adjustments and dose-response estimation of noncancer toxicity in the upper respiratory tract. *Inhal. Toxicol.* 6(suppl. l):301–325.

Jarabek, A. M. 1995a. Interspecies extrapolation based on mechanistic determinants of chemical disposition. *Hum. Ecol. Risk Assess.* 1(5):641–662.

Jarabek, A. M. 1995b. Consideration of temporal toxicity challenges current default approaches. *Inhal. Toxicol.* 7:929–946.

Jarabek, A. M. 1995c. The application of dosimetry models to identify key processes and parameters for default dose-response assessment approaches. *Toxicol. Lett.* 79:171–184.

Jarabek, A. M. 2000. *Mode of action: Framework for dosimetry model development.* Presented at Mode-of-Action Dosimetry: An Interagency Project to Develop Models for Inhalation, Oral, and Dermal Disposition, Annual Meeting of the Society for Risk Analysis, 4–6 December, Arlington, VA. Abstract available online at http://www.sra.org.

Jarabek, A. M., Ménache, M. G., Overton, J. H., Jr., Dourson, M. L., and Miller, F. J. 1989. Inhalation reference Dose (RfDi): An application of interspecies dosimetry modeling for risk assessment of insoluble particles. *Health. Phys.* 57(suppl. 1):177–183.

Jarabek, A. M., Ménache, M. G., Overton, J. H., Jr., Dourson, M. L., and Miller, F. J. 1990. The U.S. Environmental Protection Agency's inhalation RfD methodology: Risk assessment for air toxics. *Toxicol. Ind. Health* 6:279–301.

Killingsworth, C. R., Alessandrini, F., Krishna Murthy, G. G., Catalano, P. J., Paulauskis, J. D., and Godleski, J. J. 1997. Inflammation, chemokine expression, and death in monocrotaline-treated rats following fuel oil fly ash inhalation. *Inhal. Toxicol.* 9:541–565.

Kimbell, J. S., Subramaniam, R. P., Gross, E. A., Schlosser, P. M., and Morgan, K. T. 2001. Dosimetry modeling of inhaled formaldehyde: Comparisons of local flux predictions in the rat, monkey, and human nasal passages. *Toxicol. Sci*. 64:100–110.

Kimbell, J. S., Kalisak, D. L., Conolly, R. B., Miller, F. J., and Jarabek, A. M. 2004. A mechanistic model of lifetime cancer risk for inhalation exposures to reactive gases. *Toxicol. Sci.*

Koblinger, L., and Hofmann, W. 1985. Analysis of human lung morphometric data for stochastic aerosol deposition calculations. *Phys. Med. Biol*. 30:541–556.

Koblinger, L., and Hofmann, W. 1990. Monte Carlo modeling of aerosol deposition in human lungs. Part I: Simulation of particle transport in a stochastic lung structure. *J. Aerosol Sci.* 21:661–674.

Kodavanti, U. P., Schladweiler, M. C., Ledbetter, A. D., Watkinson, W. P., Campen, M. J., Winsett, D. W., Richards, J. R., Crissman, K. M., Hatch, G. E., and Costa, D. L. 2000. The spontaneously hypertensive rat as a model of human cardiovascular disease: Evidence of exacerbated cardiopulmonary injury and oxidative stress from inhaled

emission particulate matter *Toxicol. Appl. Pharmacol.* 164:250–263.

Ménache, M. G., Miller, F. J., and Raabe, O. G. 1995. Particle inhalability curves for humans and small laboratory animals. *Ann. Occup. Hyg.* 39(3):317–328.

Miller, F. J. 2000. Dosimetry of particles in laboratory animals and humans in relationship to issues surrounding lung overload and human health risk assessment: A critical review. *Inhal. Toxicol.* 12(1–2):19–58.

Miller, F. J., Martonen, T. B., Ménache, M. G., Graham, R. C., Spektor, D. M., and Lippmann, M. 1988. Influence of breathing mode and activity level on the regional deposition of inhaled particles and implications for regulatory standards. In *Inhaled particles VI: Proceedings of an international symposium and workshop on lung dosimetry* eds. J. Dodgson, R. I. McCallum, M. R. Bailey, and D. R. Fisher, September 1985, Cambridge, United Kingdom. *Ann. Occup. Hyg.* 32(suppl. 1):3–10.

Miller, F. J., Anjilvel, S., Ménache, M. G., Asgharian, B., and Gerrity, T. R. 1995. Dosimetric issues relating to particulate toxicity. In *Proceedings of the colloquium on particulate air pollution and human mortality and morbidity, Part II*, eds. R. F. Phalen and D. V. Bates, January 1994, Irvine, CA. *Inhal. Toxicol.* 7:615–632.

Miller, F. J., Schlosser, P. M., and Jansen, D. B. 2000. Haber's rule: A special case in a family of curves relating concentration and duration of exposure to a fixed level of response for a given endpoint. *Toxicologist* 149:21–34.

Morrow, P. E. 1988. Possible mechanisms to explain dust overloading of the lungs. *Fundam. Appl. Toxicol.* 10:369–384.

Moss, O. R., and Cheng, Y.-S. 1989. Generation and characterization of test atmospheres: Particles. In *Concepts in inhalation toxicology*, eds. R. O. McClellan and R. F. Henderson, pp. 85–120. New York: Hemisphere.

National Council on Radiation Protection and Measurements. 1997. *Deposition, retention and dosimetry of inhaled radioactive substances*. NCRP Report 125. Bethesda, MD: NCRP.

Oberdörster, G. 1996. Significance of particle parameters in the evaluation of exposure-dose-response relationships of inhaled particles. In *Particle overload in the rat lung and lung cancer: Implications for human risk assessment*, eds. J. L. Mauderley and R. J. McCunney, Proceedings of a conference held at the Massachusetts Institute of Technology, 29–30 March 1995, pp. 73–90. Washington DC: Taylor & Francis.

Oberdörster, G. 2002. Toxicokinetics and effects of fibrous and nonfibrous particles. *Inhal. Toxicol.* 14(1):29–56.

Oberdörster, G., Ferin, J., and Lehnert, B. E. 1994. Correlation between particle size, *in vivo* particle persistence, and lung injury. *Environ. Health Perspect.* 102(suppl. 5):173–179.

Raabe, O. G., Yeh, H.-C., Schum, G. M., and Phalen, R. F. 1976. *Tracheobronchial geometry: Human, dog, rat, hamster.* Albuquerque, NM: Lovelace Foundation, Report LF-53.

Raabe, O. G., Yeh, H.-C., Newton, G. J., Phalen, R. F., and Velasquez, D. J. 1977. Deposition of inhaled monodisperse aerosols in small rodents. In *Inhaled particles IV, Part I: Proceedings of an international symposium*, eds. W. H. Walton, and B. McGovern, September 1975, Edinburgh, Scotland, pp. 3–21. Oxford, U.K: Pergamon Press.

Raabe, O. G., Al-Bayati, M. A., Teague, S. V., Rasolt, A. 1988. Regional deposition of inhaled monodisperse, coarse, and fine aerosol particles in small laboratory animals. In *Inhaled particles VI: Proceedings of an international symposium and workshop on lung dosimetry*, eds. J. Dodgson, R. I. McCallum, M. R. Bailey, and D. R. Fischer, September, 1985, Cambridge, United Kingdom. *Ann. Occup. Hyg.* 32(suppl. 1):53–63.

Rudolf, G. 1984. A mathematical model for the deposition of aerosol particles in the human respiratory tract. *J. Aerosol Sci.* 15:195–199.

Schlesinger, R. B. 1985. Comparative deposition of inhaled aerosols in experimental animals and humans: A review. *J. Toxicol. Environ. Health* 15:197–214.

Schroeter, J. D., Musante, C. J., Hwang, D., Burton, R., Guilmette, R., and Martonen, T. B. 2001. Hygroscopic growth and deposition of inhaled secondary cigarette smoke in human nasal pathways. *Aerosol Sci. Technol*. 34:137–143.

Segal, R. A., Martonen, T. B., Kim, C. S., and Shearer, M. 2002. Computer simulations of particle deposition in the lungs of chronic obstructive pulmonary disease patients. *Inhal. Toxicol.* 14:705–720.

Snipes, M. B., James, A. C., and Jarabek, A. M. 1997. The 1994 ICRP66 human respiratory tract model as a tool for predicting lung burdens from exposures to environmental aerosols. *Appl. Occup. Environ. Hyg.* 12(8):547–554.

Stöber, W., Morrow, P. E., Koch, W., and Morawietz, G. 1994. Alveolar clearance and retention of inhaled insoluble particles in rats simulated by a model inferring macrophage particle load distributions. *J. Aerosol Sci.* 25(5):975–1002.

Stone, K. C., Mercer, R. R., Gehr, P., Stockstill, B., and Crapo, J. D. 1992. Allometric relationships of cell numbers and size in the mammalian lung. *Am. J. Respir. Cell. Mol. Biol.* 6:235–243.

Subramaniam, R. P., Asgharian, B., Freijer J. I., Miller, F. J., and Anjilvel, S. 2003. Analysis of lobar differences in particle deposition in the human lung. *Inhal. Toxicol*. 15(1):1–21.

Tran, C. L., Buchanan, D., Cullen, R. T., Searl, A., Ones, A. D., and Donaldson, K. 2000a. Inhalation of poorly soluble particles. II. Influence of particle surface area on inflammation and clearance. *Inhal. Toxicol.* 12:1113–1126.

Tran, C. L., Buchanan, D., Miller, B. G., and Jones, A. D. 2000b. Mathematical modeling to predict the response to poorly soluble particles in rat lungs. *Inhal. Toxicol.* 12(3):403–409.

U.S. Environmental Protection Agency. 1994. *Methods for derivation of inhalation reference concentrations and application of inhalation dosimetry*. Office of Research and Development, Office of Health and Environmental Assessment, Environmental Criteria and Assessment Office, Research Triangle Park, NC. Report EPA/600/8-90/066F. Final. October.

U.S. Environmental Protection Agency. 1995. *The use of the benchmark dose in health risk assessment*. Office of Research and Development, Risk Assessment Forum, Washington, DC. EPA/630/R-94/007.

U.S. Environmental Protection Agency. 1996. Dosimetry of inhaled particles in the respiratory tract In *Air quality criteria for particulate matter*, vol. II of III, chap. 10. Office of Research and Development, Washington, DC. EPA/600/P-95/001bF. April.

U.S. Environmental Protection Agency. 1999. *Revised cancer guidelines for carcinogen risk assessment*. Office of Research and Development, Risk Assessment Forum. NCEA_F-0644. External review draft.

U.S. Environmental Protection Agency. 2004. Dosimetry of particulate matter. In *Air quality criteria for particulate matter*, vol II of II, chap. 6. Office of Research and Development, Washington, DC. EPA 600P-99/002bF.

Wiltse, J. A., and Dellarco, V. L. 2000. U.S. Environmental Protection Agency's revised guidelines for carcinogen risk assessment: Evaluating a postulated mode of carcinogenic action in guiding dose-response extrapolation. *Mutat. Res.* 464:105–115.

Wolff, R. K. 1992. Mucociliary function. In *Treatise on pulmonary toxicology: Comparative biology of the normal lung*, vol. I, ed. R. A. Parent, chap, 35. Boca Raton, FL: CRC Press.

Yeh, H.-C., and Schum, G. M. 1980. Models of human lung airways and their application to inhaled particle deposition. *Bull. Math. Biol.* 42:461–480.

Yeh, H.-C., Schum, G. M., and Duggen, M. T. 1979. Anatomic models of the tracheobronchial and pulmonary regions of the rat. *Anat. Rec.* 195:483–492.

Yu, C. P. 1996. Extrapolation modeling of particle deposition and retention from rats to humans. *Inhal. Toxicol.* 8(suppl.):279–291.

Zhang, L., and Yu, C. P. 1993. Empirical equations for nasal deposition of inhaled particles in small laboratory animals and humans. *Aerosol Sci. Technol.* 19:51–56.